

# Microstructural Analysis and Enhancement of Mechanical Properties in AA2219 Composite by In-Situ $TiB_2$ and Sub-Micron $ZrB_2$ Particles

Gangaraju Moopuri\*

Department of Mechanical Engineering, Sree Vidyanikethan Engineering College (Autonomous), Tirupati, Andhra Pradesh, India.

Sharun Victor

Department of Mechanical Engineering, Panimalar Institute of Technology, Chennai, Tamilnadu, India.

Michael Raj Francis

Department of Mechanical Engineering, Stella Mary's College of Engineering, Aruthenganvilai, Tamilnadu, India.

## Abstract

Composite material technology was created to maximize the beneficial features of metallic and ceramic materials. Among the numerous processing approaches, flex aided synthesis is a high-potential, low-cost way for generating in-situ composites. In-situ aluminium matrix composites outperform ex-situ composites due to the chemically dispersed reinforcements. The current work employs a flex assisted synthesis process to create AA2219 -  $TiB_2/ZrB_2$  in-situ aluminium matrix composites with varying reinforcement ratios. The presence of reinforcement and the element percentage of the composites are confirmed by EDAX analysis. Also, morphological analysis revealed the dispersal of in-situ reinforcements and  $CuAl_2$  creation in the matrix's grain border areas. Moreover, the presence of 4% optimum reinforcement was revealed by the increase in hardness, compressive strength, tensile strength and corrosion resistance for the composites over AA2219 matrix.

**Keywords:** AA2219 Aluminum Alloy,  $TiB_2/ZrB_2$ , EDAX, SEM, Micro hardness.

## 1. Introduction

Many researchers are attentive in aluminium matrix composites because of their enhanced mechanical properties and wear resistance while being its lightweight. In the automotive industry, these composites are employed to make pistons, engine blocks, disc rotor brakes, drums and connecting rods [1]. Metal matrix composites invented in-situ have received a lot of attention due to their superior performance. The conventional method for manufacturing metal matrix composites results in an uneven distribution of reinforcement, poor wetting, reinforcement agglomeration, and low interfacial strength [2]. The application of reinforcement particulates to the molten matrix limits this technology. In the in-situ technique, the reinforcement is formed in the host matrix via a chemical reaction between the matrix and the reinforcements [3]. This method results in a thermodynamically stable, chemically pure reinforcement phase. Numerous advantages of these composites include enhanced bonding strength, fineness, lack of agglomeration, and uniform reinforcement distribution. Mechanical properties such as strength and stiffness are significantly increased as a result [4-6]. Aluminum alloy AA2219 is a high-strength aluminium alloy that is frequently used in aerospace applications such as cryogenic rocket fuel tanks and lightweight structures. Its weldability, strength-to-weight ratio, corrosion resistance, and cryogenic properties are all improved [7-9]. Composites with a metallic matrix and a hard ceramic reinforcement are called metal matrix composites. Due to the addition of an additional reinforcement phase, they are hybrid composites. Multiple ceramic particle reinforced composites are being developed to achieve properties that a single ceramic material cannot achieve [7].

Wang et al. [10] synthesized a  $Al/(TiC+-Al_2O_3)$  and  $Al/(TiAl_3+TiC+-Al_2O_3)$  alloys are formed in situ when Al,  $TiO_2$ , and C react in liquid aluminium. The results indicate that TiC particles are spherical in shape and range in size between 0.3 and 1.5  $\mu m$ ;  $-Al_2O_3$  particles are polyhedral in shape and range in size between 1 and 3  $\mu m$ . Zhao et al. [11] synthesized multiple ceramic particle reinforced MMCs using flex assisted synthesis.  $K_2ZrF_6-K_2TiF_6-KBF_4$  A starting material system is used to generate in-situ  $TiB_2$  and  $ZrB_2$  particles. The results of the microstructural analysis indicate that the  $TiB_2$  and  $ZrB_2$  reinforcement particles are distributed uniformly throughout the aluminium matrix. Additionally, it was determined that the average  $TiB_2$  particle size is approximately 1  $\mu m$ , while the average  $ZrB_2$  particle size is approximately 0.3  $\mu m$ . S.C. Tjong and G.S. Wang [9] proposed a novel method for the fabrication of hybrid ceramic composites based on the  $Al-TiO_2-B$  and  $Al-TiO_2-B_2O_3$  material systems. Using an  $Al-TiO_2-B_2O_3$  material system, Xing et al [10] used an in-situ reaction to create an aluminium matrix composite reinforced with  $TiB_2/Al_2O_3$  ceramic particles. After spray deposition, they used a hot-press treatment technique.

Wang et al. [12] synthesised multiple  $TiB_2-TiC-Al_2O_3$  ceramic particles in situ. They have used gas tungsten arc welding to reinforce Fe-based composite coatings and discovered that  $TiB_2$  particles have a blocky morphology. The TiC particles are shaped like flowers, whereas the  $Al_2O_3$  particles are small black dots found within reinforced particles. A hard composite coating reinforced

with TiB<sub>2</sub>-TiC was created on steel using laser deposition, and it was discovered that micron-sized blocky particles and sub-micron-sized spherical particles are used as reinforcements [13]. This article's primary contribution is an investigation of the effect of multiple ceramic reinforcements TiB<sub>2</sub> and ZrB<sub>2</sub> formed in situ on an Al-Cu-Mn alloy. This research describes the synthesis, quantitative elemental analysis, microstructure characteristics, and microhardness analysis of these composites.

## 2. Material synthesis of hybrid composites

The chemical composition of AA2219, an Al-Cu-Mn ternary alloy system is given in the Table 1. To create composites, the flex assisted synthesis method is used as well as the matrix material AA2219 was used. The TiB<sub>2</sub> and ZrB<sub>2</sub> reinforcements were synthesized using three different halide salts: potassium hexa fluorotitanate (K<sub>2</sub>TiF<sub>6</sub>), potassium hexa fluorozirconate (K<sub>2</sub>ZrF<sub>6</sub>), and potassium tetra fluoroborate (KBF<sub>4</sub>). Table 2 shows the number of materials needed to make the composite.

**Table 1:** Chemical arrangement (Wt. %) of base metal

Material	Cu	Mn	Fe	Zr	V	Si	Ti	Zn	Al
Wt. %	6.33	0.34	0.13	0.12	0.07	0.06	0.04	0.02	Bal

**Table 2:** Essential raw materials for composite fabrication

S.No	Materials	Quantity (Grams)				
		0% TiB <sub>2</sub> /ZrB <sub>2</sub>	2% TiB <sub>2</sub> /ZrB <sub>2</sub>	4% TiB <sub>2</sub> /ZrB <sub>2</sub>	6% TiB <sub>2</sub> /ZrB <sub>2</sub>	8% TiB <sub>2</sub> /ZrB <sub>2</sub>
1	AA2219	2250	2250	2250	2250	2250
2	K <sub>2</sub> TiF <sub>6</sub>	Nil	20	40	60	80
3	K <sub>2</sub> ZrF <sub>6</sub>	Nil	50	60	70	80
4	KBF <sub>4</sub>	Nil	30	40	60	80



**Figure 1:** AA2219 Aluminum Alloy Matrix Composite

During the synthesis, the preheated halide salts were introduced into the aluminium alloy melt (figure 1) at a temperature of 850°C. About 15 minutes later, the melt is stirred and allowed to react chemically. When molten aluminium alloy reacts with halide salts, exothermic reactions occur, releasing temperatures of up to 1300°C. As a result of this exothermic reaction, TiB<sub>2</sub> and ZrB<sub>2</sub> particulates are formed and dispersed within the aluminium grain boundaries. The chemical reaction results in the formation of KAlF<sub>4</sub> and K<sub>3</sub>AlF<sub>6</sub>, which are then removed as slag. The molten composite is then poured into a graphite-coated cast iron mould.

### 3. Results and Discussions

#### 3.1. Fatigue Strength of AA2219 Composite

**Table 3:** Fatigue strength of Composite

Composites	Fatigue Strength (MPa)			
	Trail I	Trail II	Trail III	Average
AA2219-0% TiB <sub>2</sub> /ZrB <sub>2</sub>	104	105	104	104.33
AA2219-2% TiB <sub>2</sub> /ZrB <sub>2</sub>	108	107	110	108.33
AA2219-4% TiB <sub>2</sub> /ZrB <sub>2</sub>	111	113	114	112.67
AA2219-6% TiB <sub>2</sub> /ZrB <sub>2</sub>	109	108	109	108.67
AA2219-8% TiB <sub>2</sub> /ZrB <sub>2</sub>	107	109	108	108.00

The fatigue strength was evaluated for the prepared composites as listed in Table 3. It was found that increase in the fatigue strength of developed composites was found till the combination A2219-4% TiB<sub>2</sub>/ZrB<sub>2</sub> reaching a value 112.67 MPa and further improvement in the reinforcement had led to decline in the properties of fabricated composites due to formation of agglomeration and non-uniformity of the matrix mixtures in the developed composite. However, the optimum composition identified as AA2219-4% TiB<sub>2</sub>/ZrB<sub>2</sub> confirms the uniform mixture of composites and thereby withstands more fatigue failure resulting in better properties.

#### 3.2. Micro Hardness of AA2219 Composite

The Vickers micro hardness tester MH06 model (CECRI, Karaikudi, India) was used to evaluate the hardness of composites at a load of 25 gm and a dwell time of 3 sec. The Vickers micro hardness value for all the combination of composites developed in AA2219 alloy with an additional reinforcement from 2% to 8 % with an increment of 2% is shown in Table 4. The addition of reinforcements to AA2219 alloy increases the material hardness. In view to the text, the presence of 4% reinforcement in AA2219 alloy had raised the hardness from 122 to 155 owing to the uniform distribution of reinforcement with the matrix material in the fabricated composites and further enhancement of reinforcement resulted in decline trend of hardness. This phenomenon may be due to the mixing issues and agglomeration raised during the preparation of matrix reinforcement solution.

**Table 4:** Determined Micro Hardness

Composites	Micro hardness (Hv)			
	Trail I	Trail II	Trail III	Average
AA2219-0% TiB <sub>2</sub> /ZrB <sub>2</sub>	122	125	119	122
AA2219-2% TiB <sub>2</sub> /ZrB <sub>2</sub>	148	143	139	143
AA2219-4% TiB <sub>2</sub> /ZrB <sub>2</sub>	156	152	159	155
AA2219-6% TiB <sub>2</sub> /ZrB <sub>2</sub>	152	150	153	151
AA2219-8% TiB <sub>2</sub> /ZrB <sub>2</sub>	149	151	148	149

#### 3.3. Tensile Strength of AA2219 Composite

**Table 5:** Tensile strength of Composite

Composites	Tensile Strength (MPa)			
	Trail I	Trail II	Trail III	Average
AA2219-0% TiB <sub>2</sub> /ZrB <sub>2</sub>	273	276	274	274.33
AA2219-2% TiB <sub>2</sub> /ZrB <sub>2</sub>	281	283	286	283.33
AA2219-4% TiB <sub>2</sub> /ZrB <sub>2</sub>	304	307	309	306.67
AA2219-6% TiB <sub>2</sub> /ZrB <sub>2</sub>	297	298	296	297.00
AA2219-8% TiB <sub>2</sub> /ZrB <sub>2</sub>	293	296	294	294.33

The tensile strength evaluated for the prepared hybrid composites is shown in Table 5. Similar trend as noticed in fatigue and tensile strength of the developed composite was observed here. The minimum tensile strength attained was 274.33 MPa for AA2219-0% TiB<sub>2</sub>/ZrB<sub>2</sub> and further addition of the incorporated reinforcements from 2 % to composite showed an increase of strength up to AA2219-4% TiB<sub>2</sub>/ZrB<sub>2</sub> (306.67 MPa), whereas the addition of reinforcement beyond this limit had resulted in weakening of hybrid composites leading to decreased characteristics. This may be due to the poor interfacial bonding features between the matrix and reinforcement when applied to tensile loads.

### 3.4. Compressive Strength of AA2219 Composite

Similarly, the compressive strength of developed AA2219 TiB<sub>2</sub>/ZrB<sub>2</sub> hybrid composites exhibited a trend alike to all properties. It was clearly evident and revealed that the optimum composition suit for this novel hybrid composite was AA2219-4% TiB<sub>2</sub>/ZrB<sub>2</sub> where more withstanding capacity of the compressive load was noticed as represented in Table 6 due to uniform distribution of reinforcement and good bonding features with the matrix. However, the composites made using other combinations explored the failure behaviors owing to the interfacial bonding features and brittleness nature occurred in the middle of the composites during compressive loading.

**Table 6:** Compressive strength of composite

Composites	Compressive Strength (MPa)			
	Trail I	Trail II	Trail III	Average
AA2219-0% TiB <sub>2</sub> /ZrB <sub>2</sub>	152	153	152	152.33
AA2219-2% TiB <sub>2</sub> /ZrB <sub>2</sub>	159	159	158	158.67
AA2219-4% TiB <sub>2</sub> /ZrB <sub>2</sub>	164	166	163	164.33
AA2219-6% TiB <sub>2</sub> /ZrB <sub>2</sub>	161	163	163	162.33
AA2219-8% TiB <sub>2</sub> /ZrB <sub>2</sub>	158	161	159	159.33

### 3.5. Weight Loss calculation of AA2219 Composite

**Table 7:** Weight Loss of Composite

Composites	In Months & Weight Loss in grams			
	1	2	3	4
AA2219-0% TiB <sub>2</sub> /ZrB <sub>2</sub>	0.1	0.12	0.13	0.16
AA2219-2% TiB <sub>2</sub> /ZrB <sub>2</sub>	0	0.08	0.08	0.09
AA2219-4% TiB <sub>2</sub> /ZrB <sub>2</sub>	0	0	0	0.02
AA2219-6% TiB <sub>2</sub> /ZrB <sub>2</sub>	0	0	0.01	0.03
AA2219-8% TiB <sub>2</sub> /ZrB <sub>2</sub>	0	0	0.01	0.02

$$\text{Weight Loss in \%} = \frac{\text{Initial Weight} - \text{Final Weight}}{\text{Initial Weight}} \times 100 \quad - (1)$$

The general weight loss method was used to identify the corrosion resistance of the fabricated composites specimens under natural sea water using the standard equation (1). The specimens were evaluated for the duration of 1 to 4 months (120 days) and the observed values were displayed in Table 7. It was observed that AA2219-4% TiB<sub>2</sub>/ZrB<sub>2</sub> incorporated composites can withstand more corrosion resistance subjected to the immersion of specimen under sea water when compared with other fabricated specimens.

### 3.6. Quantitative elemental analysis of AA2219 composite

The EDAX analysis was performed on a Hitachi S-300H model (CECRI, Karaikudi, India). The EDAX spectra of samples were acquired using a lithium drift silicon detector analyzer operating at a voltage of 20KV and a magnification of 500X. The EDAX spectra of AA2219-2% TiB<sub>2</sub>/ZrB<sub>2</sub> and AA2219-4% TiB<sub>2</sub>/ZrB<sub>2</sub> in Figure 2a and 2b represent the composition of various elements present in composites, respectively.

The recognition of aluminium, copper, titanium boride and zirconium boride elements in the sample is shown in fig. 2a and fig.2b. The elements Mn and V which are extant in the AA2219 alloy are represented by the other small peaks. Table 8 correspond to AA2219- 2% TiB<sub>2</sub>/ZrB<sub>2</sub> clearly represents that the wt.% of Al, Cu, Ti and Zr as 91.83, 4.92, 1.86 and 1.39 respectively. However, the Table 9 representing AA2219- 4% TiB<sub>2</sub>/ZrB<sub>2</sub> sample contained Al, Cu, Ti and Zr as 87.8, 5.27, 4.42 and 2.51 revealing the difference in percentage of parent metal aluminium when addition in reinforcement was done. The major elements will be oxidized during synthesis due to the high temperatures generated by the chemical reaction, whereas the presence of Ti and Zr elements existing in the AA2219 alloy will reimburse for projected composition.

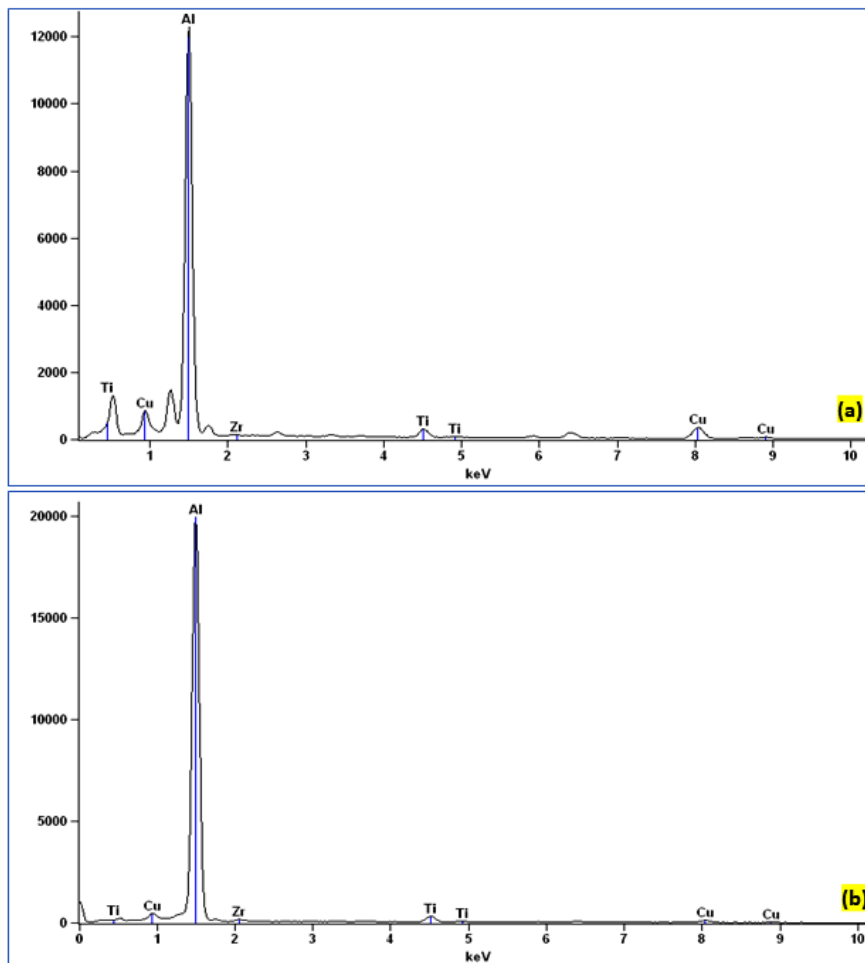


**Figure 2:** EDAX spectrum: a) AA2219- 2% TiB<sub>2</sub>/ZrB<sub>2</sub> and b) AA2219- 4 % TiB<sub>2</sub>/ZrB<sub>2</sub>

**Table 8:** Measurable Elemental Study of AA2219- 2% TiB<sub>2</sub>/ZrB<sub>2</sub>

Element	Net Counts	Weight %	Atom %
Al	122517	91.83	94.43
Cu	3521	4.92	2.93
Ti	1762	1.86	1.24
Zr	724	1.39	1.4
Total		100.00	100.00

**Table 9:** Measurable Elemental Study of AA2219- 4 % TiB<sub>2</sub>/ZrB<sub>2</sub>

Element	Net Counts	Weight %	Atom %
Al	210741	87.8	93.86
Cu	2177	5.27	2.46
Ti	4232	4.42	2.7
Zr	1948	2.51	0.98
Total		100.00	100.00

### 3.7. Microstructure analysis of AA2219 composite

The scanning electron microscope JEOL6360 LV Model was used to capture the micrographs (P.S.G.Tech, Coimbatore, India). Meanwhile, fine emery sheets are used to polish the composites and Keller's solution is used to etch them. Figure 3a depicts the microstructure of the AA2219 alloy and the occurrence of copper in AA2219 alloy results in fine CuAl<sub>2</sub>. Also, in the grain boundaries of aluminium alloy, homogeneous formation of copper melts (CuAl<sub>2</sub>) occurs. However, figure 3b showing the SEM micrograph of AA2219- 6 % TiB<sub>2</sub>/ZrB<sub>2</sub> composite at 200X magnification revealed the interdendritic regions, reinforcements and formation of CuAl<sub>2</sub>. In addition, the interfacial integrity amid the reinforcements, CuAl<sub>2</sub> and the aluminium matrix was found good. Figure 3c depicts a miniscule view of the interdendritic region of an AA2219-4% TiB<sub>2</sub>/ZrB<sub>2</sub> composite showing the distribution of TiB<sub>2</sub> and sub-micron ZrB<sub>2</sub> reinforcement. Over 5000 X magnification, these reinforcement particles are focused and observed that TiB<sub>2</sub> has an average size of around 1, whereas ZrB<sub>2</sub> has an average size of 0.7. As a result of better properties, this microstructure study revealed that there is no noticeable boundary perceived in the microstructure.

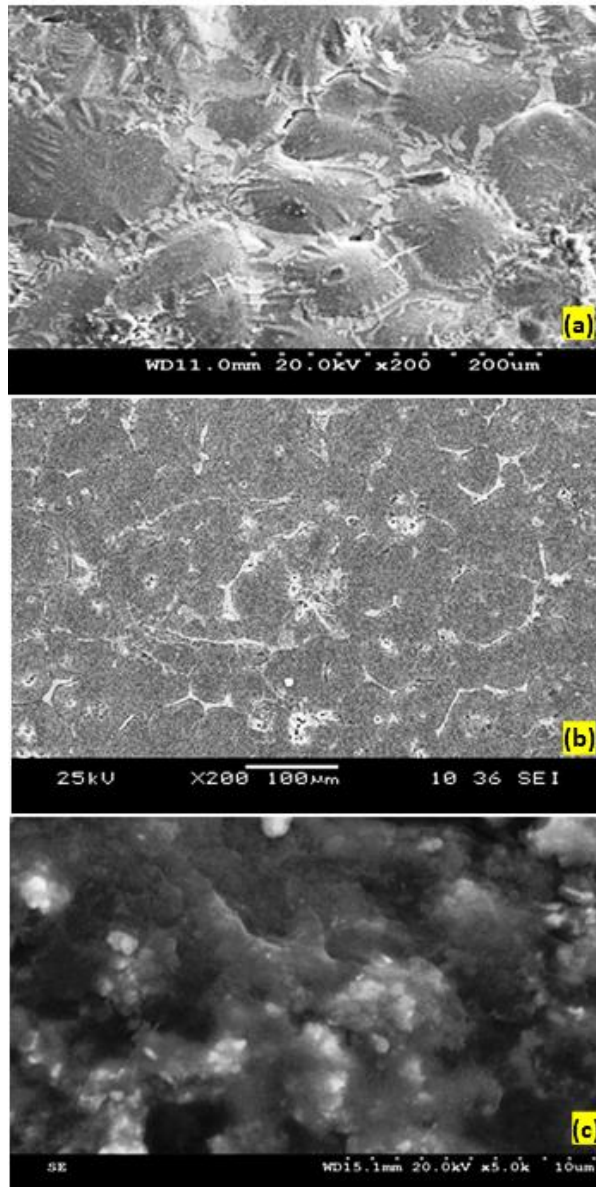


**Figure 3:** Microstructural photograph a) AA2219 alloy b) AA2219- 6 % TiB<sub>2</sub>/ZrB<sub>2</sub> and c) AA2219- 4 % TiB<sub>2</sub>/ZrB<sub>2</sub> composite

#### 4. Conclusions

The AA2219 - TiB<sub>2</sub>/ZrB<sub>2</sub> in-situ composite was successfully synthesized using the flex assisted synthesis method. EDAX analysis confirmed the presence of multiple ceramic reinforcements. According to quantitative elemental analysis, the element percentages of composites are in good contract with those of their particular parent materials. The elements like CuAl<sub>2</sub>, TiB<sub>2</sub> and ZrB<sub>2</sub> formed by in-situ chemical reactions are found in the grain limit regions of aluminium matrix examined by microstructural analysis. The addition of reinforcements to the 4% AA2219 matrix identified as optimum composition resulted in showing a significant increase in hardness, compressive strength, tensile strength and corrosion resistance. Moreover, the composite made using optimum combination revealed that there is no detectable interface in the composite making it suit for diverse applications.

#### Author Contributions

G.M.: conceptualization, investigation, reviewing and editing; S.V.: investigation, methodology, writing an original draft; M.R.F.: research design, data analysis; data curation, writing-reviewing and editing, project administration. All authors have read and agreed to the published version of the manuscript.

#### Conflicts of Interest

The authors declare no conflict of interest.

## References

1. S.V. Prasad, and R. Asthana, "Aluminum metal–matrix composites for automotive applications: tribological considerations," *Tribology Letters*, vol. 17, pp.445 - 453, 2004.
2. E.Zhang, S.Zeng, B.Yang, and Q.Li, "Microstructure and mechanical properties of in-situ Al-Cu/TiC composites," *Journal of Material Science Technology*, vol.14, pp. 255- 258, 1998.
3. R. M. Aikin, "The mechanical properties of in-situ composites," *JOM Journal of the Minerals*, vol.49, pp.35-39, 1997.
4. C. Cui, Y. Shen, and F.Meng, "Review on fabrication methods of in-situ metal matrix composites", *Journal of Material Science Technology*, vol.16, pp. 619-626, 2000.
5. P Srinivasa Rao, K G Sivadasan and P K Balasubramanian, "Structure-property correlation on AA 2219 aluminum alloy weldments", *Bulletin of Materials Science*, vol.19 , pp. 549-557,1996.
6. S.Babu, K.Elangovan, V. Balasubramanian, and M.Balasubramanian, "Optimizing friction stir welding parameters to maximize tensile strength of AA2219 aluminum alloy joints", *Met. Mater. Int.*, vol. 15, pp. 321-330, 2009.
7. G. Peter, J. Livin, and A. Sherine, "Hybrid optimization algorithm based optimal resource allocation for cooperative cognitive radio network," *Array*, vol. 12, p. 100093, Dec. 2021, doi: 10.1016/j.array.2021.100093.
8. Z. Wang and X. Liu , "In-situ synthesis of Al/(TiC+ $\alpha$ -Al<sub>2</sub>O<sub>3</sub>) and Al/(TiAl<sub>3</sub>+TiC+ $\alpha$ -Al<sub>2</sub>O<sub>3</sub>) alloys by reactions between Al, TiO<sub>2</sub> and C in liquid aluminum", *Journal of Materials Science*, vol. 40, pp.1047-1050, 2005.
9. D. Zhao, X. Liu, Y. Liu, and X. Bian, "In-situ preparation of Al matrix composites reinforced by TiB<sub>2</sub> particles and sub-micron ZrB<sub>2</sub>", *Journal of Material Science*, vol.40, pp.4365-4368, 2005.
10. G. Peter and S. Bin Iderus, "Design of enhanced energy meter using GSM prepaid system and protective relays," *Materials Today: Proceedings*, vol. 39, pp. 582–589, 2021, doi: 10.1016/j.matpr.2020.08.471.
11. M. Sambathkumar, P. Navaneethkrishnan, K. Ponappa, K.S.K. Sasikumar "Analysis of Al7075 Hybrid Metal Matrix Composite Using Two Dimensional Microstructure Model Based Finite Element Method", *International Journal of Advanced Engineering Technology*, vol. 7, pp.180-183, 2016.
12. D M Nuruzzaman, F F B Kamaruzaman "Processing and mechanical properties of aluminium-silicon carbide metal matrix composites", *J Materials Science and Engineering*, vol. 114, pp.142-149, 2016.
13. V.Ramakoteswara Rao,N.Ramanaiah, M.M.Sarcar, "Tribological properties of Aluminium Metal Matrix Composites", *International Journal of Advanced Science and Technology*, vol.88, pp.13-26, 2016.